

SUB-PICOSECOND BEAM PRODUCTION FOR EXTERNAL INJECTION INTO PLASMA EXPERIMENTS

O. Mete-Apsimon*, R. Apsimon and G. Burt, Lancaster University, Lancaster, UK
 G. Xia, The University of Manchester, Manchester, UK
 also at The Cockcroft Institute of Accelerator Science and Technology, Warrington, UK

Abstract

Applications of plasmas in accelerators benefit from short probe bunches comparable to plasma wavelength due to currently achievable plasma wake profiles. In plasma acceleration case, high capture efficiency within a narrow energy spectrum can be achieved when a sub-picosecond to femtosecond witness bunch injected behind the driver pulse at the high electric field region. A start-to-end simulation study was performed for parametric optimisation of an rf photoinjector to provide a short witness bunch for plasma applications in accelerators. An rf photoinjector is a laser-driven, high brightness and robust electron source that can provide stability and flexibility provided by today's advanced laser and rf technologies.

INTRODUCTION

Laser pulses (LWFA) [1, 2] or high quality short particle beams (PWFA) [3–5] are used in order to drive the plasma electrons to induce high wake fields in the plasma. LWFA occurs under the effect of the ponderomotive force of the laser pulse whereas PWFA utilises the Coulomb force between the driver beam and the plasma electrons. For PWFA the resulting wakefield strength is inversely proportional to square of the driver bunch length. Such bunches can be injected into the plasma from an external source or can be formed inside the plasma by modulation at the plasma frequency thanks to a phenomenon called self modulation instability (SMI) [6].

As well as the driver beam, the witness or the probe beam can be generated either from an external source or from the plasma itself using schemes such as ionisation injection [7–13]. There are also studies on using an LWFA as an injector for a secondary plasma channel for acceleration [14]. Magnetic undulators can also be used to microbunch an initial beam to produce a train of ultra-short bunches. A previous study demonstrated wakefield build-up as a result of such a train when compared to a single bunch case [15]. The initial quality and characteristics of a beam coupled to plasma components will aid the suitability of the final beam for the applications such as FELs or future collider design studies.

This paper discusses the production of sub picosecond electron beams from a photoinjector using conventional S-band and X-band RF structures to have hybrid frequency gun-linac layouts [16] operating at off-crest phases. A photoinjector is an electron source that uses laser pulses in order

to extract electrons from the surface of a metallic or a semiconductor cathode (such as Cu and Cs₂Te). Electrons can escape cathode surface if the laser pulses provide sufficient energy for electrons to overcome the potential barrier of the surface. Cathode plug is placed in one end of an RF gun which is used for rapid acceleration of electrons emitted from the cathode into a large solid angle. Further acceleration of the beam can be achieved by using a linac after the RF gun. Photoinjectors are used as a mature technology for electron beam production since they first implemented in 1980s. They can produce high brightness, low emittance electron beam motivating photoinjectors as versatile and reliable electron sources. Some historical highlights and overview of photoinjectors can be found in [17–19].

RF GUN OPTIONS

Beam dynamics under the accelerating and focusing fields were performed with the particle-in-cell code PARMELA [20]. External fields can be imported as field maps or generated by using the built-in models in PARMELA. For a travelling wave structure two field maps must be provided; one produced with Neumann boundary condition (cosine map) and the other with Dirichlet boundary condition (sine map). These fields which are shifted in phase by 90° are fed into PARMELA by using the TRWCFIELD command. In order to implement the PARMELA built-in model, all the cells in a structure are defined using TRWAVE cards. The fringe fields in the entrance and the exit of the structure can be modelled using a combination of half CELL and TRWAVE combination. In this study, 2D field maps for standing wave RF guns are produced by SUPERFISH [21] and provided for simulations whereas the PARMELA built-in model is used to produce the fields for the travelling wave linacs.

Simulations for an S-Band Gun

The S-band (2.99855 GHz) PHIN gun is considered as a reference representing the conventional technology for this study [22]. The gun with 2 + 1/2 cells induces 100 MV/m average axial electric field at π -mode to capture and extract the particles.

Figure 1 shows the behaviour of the rms beam energy as a function of RF phase. Please note that all phase values in this manuscript are related to the simulation master clock and arbitrary. Parabolic regions represent the typical energy behaviour around the wave crest where there is a reasonable amount of particle transmission across the gun. Rms values dip down to zero where most of the particles are lost in the process without being captured by the RF field. A working

* Now at The University of Manchester,
 oznur.mete@manchester.ac.uk

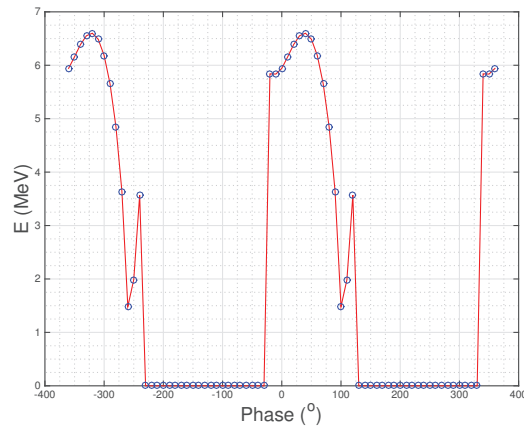


Figure 1: Rms beam energy evolution in the S-band RF gun as a function of RF phase.

point within the parabolic regions can be chosen taking into account various beam dynamics observables as well as the energy.

The number of macro-particles propagating until the exit of the RF gun, through a 20 mm aperture (radius), is presented in Fig. 2-a. The region between -5° and 95° , where there is a reasonable flat-top, will be called the transmission band. Normalised beam emittance, $\epsilon_{n,x,z}$, beam sizes, $\sigma_{x,z}$, in horizontal and longitudinal plane, respectively; rms beam energy, E and rms spread on the energy, $\Delta E/E$ can be characterised within the transmission band. Figure 2-b summarises this characterisation.

Horizontal normalised rms emittance is relatively constant around 2 mm mrad up to about 50° . The rms value starts increasing due to the loss of some particles after this point. A compromise between the rms energy and the bunch length will determine the baseline for the gun exit. In the transmission band, the bunch length is compressed for the lower phase values.

Consequently, an energy output value of 6.5 MeV was chosen as an example case which occurs at 30° and where the bunch length is 2.8 ps. An initial 4 ps (4° of RF wave) long laser pulse with a radius of 0.5 mm is used for the S-band simulations.

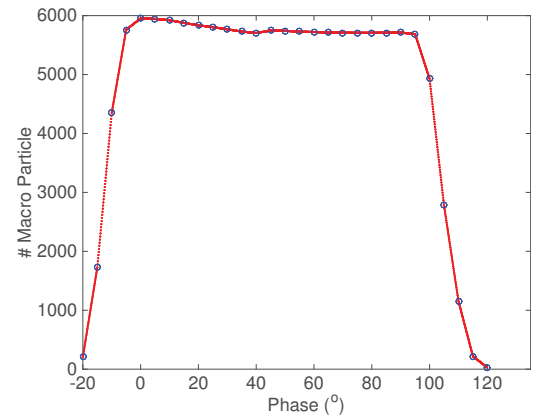
Simulations for an X-Band Gun

An X-band (11.994 GHz) RF gun with $5 + 1/2$ cells and 4 mm iris aperture (radius) was designed operating with 200 MV/m average axial electric field. Similar structures were studied before in [23, 24]. This is summarised in Fig. 3. In the case of an RF gun at X-band frequency, the same energy output of 6.5 MeV as the S-band gun was achieved at 8° resulting into a nearly 1/3 lower bunch length of 101 fs. An initial 232 fs (1° of RF wave) long laser pulse with a radius of 0.5 mm is used for the S-band simulations.

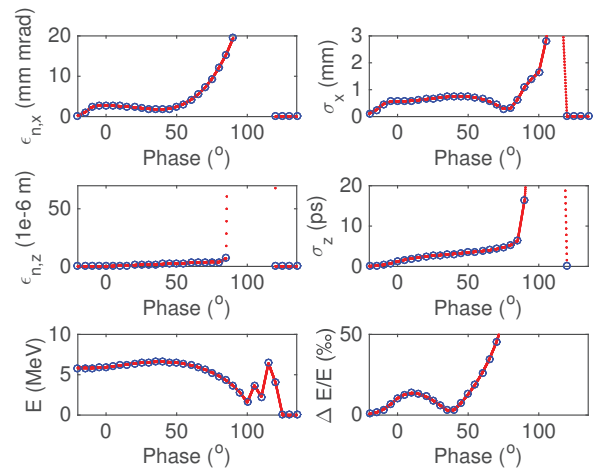
HYBRID-BAND INJECTOR

Reference case: S-S-Band

A constant gradient travelling wave linac with 15 MV/m was implemented after the S-band RF gun in order to boost



(a)



(b)

Figure 2: For the S-band RF gun; a) number of macro-particles extracted at the end of the RF gun out of 6k macro-particles and b) beam dynamics observables as a function of RF phase.

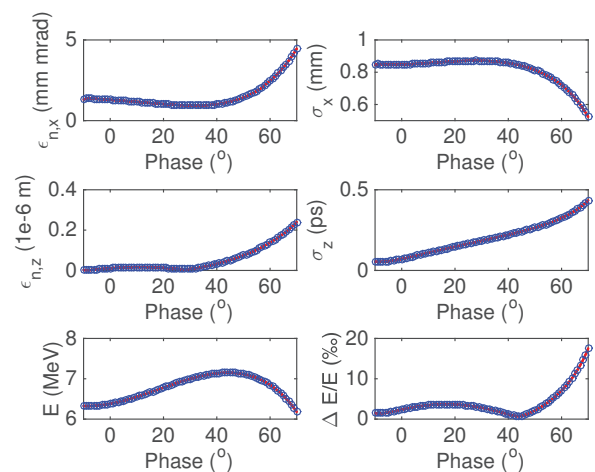


Figure 3: Beam dynamics observables as a function of RF phase at the exit of an X-band RF gun within the transmission band with 100% transmission.

to beam energy up to 15 MeV reference energy. Characterisation of the beam after the S-band linac is given in Fig. 4;

sub plot a) reveals that number of macroparticles leaving the RF gun is conserved through the linac at the transmission regions. In the first transmission region at -330° , 2.68 ps bunch length is produced at an energy of 15 MeV about 30° before the wave crest. The normalised transverse emittance is ~ 2.5 mm mrad in this region. One should note that emittance compensation was not optimised for these results hence it can still be improved.

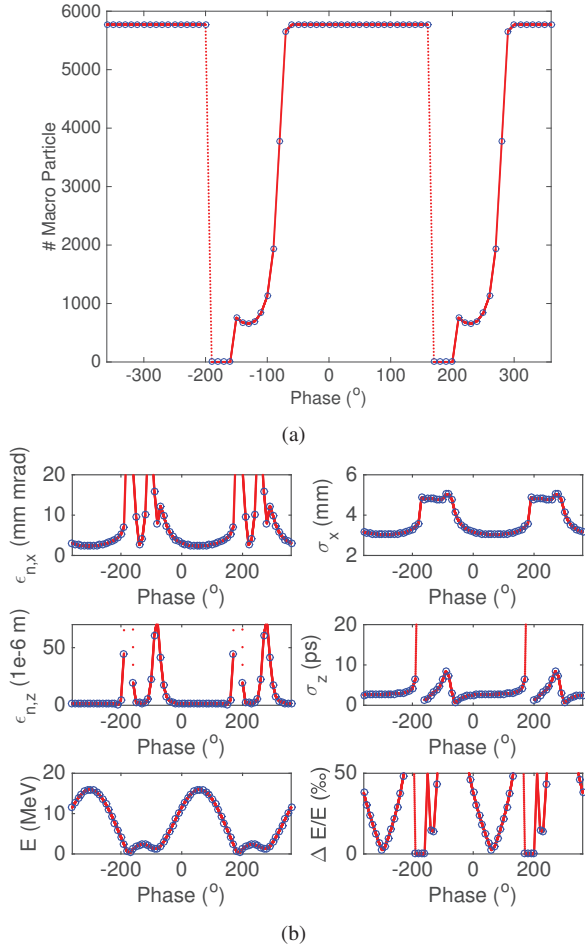


Figure 4: For the S-band RF gun and linac combination; a) number of macro-particles extracted at the end of the RF gun out of 6k macro-particles; b) beam dynamics observables as a function of RF phase.

Hybrid case: X-S-Band

Hybrid case consists of the X-band RF gun followed by the S-band linac given in previous sections. The beam dynamics observables are summarised in Fig. 5. By only upgrading the RF gun frequency, the injector can produce 95 fs bunch length at the same energy (15 MeV) and bunch charge (0.2 nC) at an RF phase of 60° , which is 30° before the wave crest. A normalised transverse beam emittance of ~ 2 mm mrad is achievable before any beam envelope optimisation. In addition, further studies are needed to investigate the effect of space charge parametrisation in PARMELA for short bunches to reliably determine the emittance. Charge extraction capability of X-band RF gun was proven better

than the S-band with full transmission within the transmission regions as a function of RF phase (Fig. 5-a).

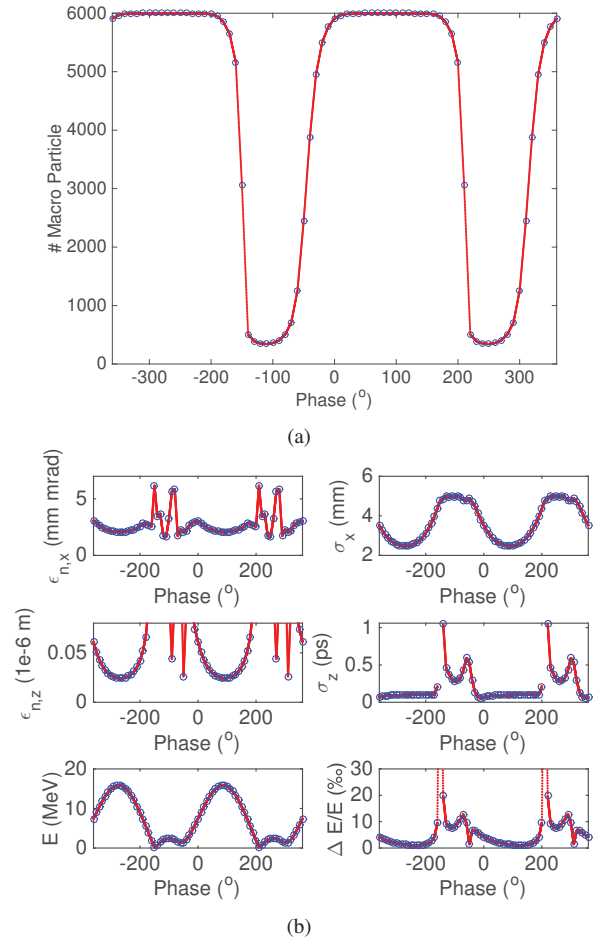


Figure 5: For the X-band RF gun and S-band linac combination; a) number of macro-particles extracted at the end of the RF gun out of 6k macro-particles; b) beam dynamics observables as a function of RF phase.

CONCLUSIONS AND FURTHER STUDIES

Short bunch production capabilities of well known S-band technology and X-band technology were compared. An X-band RF gun was numerically proven to provide better electron capturing efficiency of the macroparticles emerging from the cathode; as well as providing 30 times shorter bunches at the gun exit. Followed by an S-band linac, while S-band gun can reduce the bunch length to 2.68 ps, X-band gun managed to produce a bunch length of 95 fs. Further studies are ongoing for a fully X-band system and further space charge compensation in order to produce lower transverse emittance values.

ACKNOWLEDGMENT

This work is supported by the Cockcroft Institute Core Grant and STFC. Authors would like to thank to Mr Julian McKenzie (ASTeC) and Dr Steffen Doebert (CERN) for their comments and suggestions.

REFERENCES

- [1] E. Esarey and C. B. Schroeder, LBNL Report, LBNL-53510 (2003).
- [2] S. Steinke et al., Nature 530, 190-193 (2016).
- [3] A. Caldwell et al., CERN-SPSC-2013-013 (2013).
- [4] M. J. Hogan et al., New Journal of Physics 12, 055030 (2010).
- [5] M. E. Conde et al., Proc. of IPAC2014, TUPME058 (2014).
- [6] K. Lotov, Physics of Plasmas 22, 103110 (2015).
- [7] M. Chen et al., J. Appl. Phys. 99, 056109 (2006).
- [8] C. McGuffey et al., Phys. Rev. Lett. 104, 025004 (2010).
- [9] A. Pak et al., Phys. Rev. Lett. 104, 025003 (2010).
- [10] C. E. Clayton et al., Phys. Rev. Lett. 105, 105003 (2010).
- [11] M. Chen et al., Phys. Plasmas 19, 033101 (2012).
- [12] C. Thaury et al., Sci. Reports 5, 16310 (2015).
- [13] B. Hidding et al., AIP Conference Proc. 1507(1):570 (2012).
- [14] P. Muggli et al., Proc. of IPAC2014, TUPME048 (2014).
- [15] O. M. Apsimon, Proc. of IPAC2016, WEPMY025 (2016).
- [16] S. Doeberl, Proc. of LINAC16, THOP11 (2016).
- [17] S. J. Russell, NIMA A 507, 304 (2003).
- [18] M. Ferrario, Procs. of EPAC 2006, Scotland (2006).
- [19] L. Faillace, Physics Procedia 52, 100 (2014).
- [20] L. M. Young, LA-UR-96-1835 (2005).
- [21] K. Halbach and R. F. Holsinger, Part. Acc. 7, 213-222 (1976).
- [22] O. Mete et al., PRSTAB 15, 022803 (2012).
- [23] Y. Sun et al., PRSTAB 15, 030703 (2012).
- [24] C. Limborg-Deprey et al., PRAB 19, 053401 (2016).